SCANNING ELECTRON MICROSCOPIC STUDY OF ZnO CRYSTALLITES

A. Jishiashvili [1], Z. Shiolashvili [1], D. Jishiashvili [1, 2, *], N. Makhatadze [1], A. Chirakadze [1], V. Gobronidze [1]

[1] V. Chavchanidze Institute of Cybernetics
Georgian Technical University
Tbilisi, Georgia
* d_jishiashvili@gtu.ge
[2] E. Andronikasvili Institute of Physics
I. Javakhishvili Tbilisi State University
Tbilisi, Georgia

Accepted 2020 December 22

Abstract

The wide band-gap semiconductor – zinc oxide finds broad applications due to its unique electrical, optical, and biomedical properties. This work deals with a new method of synthesis. Scanning electron microscopy was used to study the morphology and composition of a layer produced on the Si substrate after deposition of volatile species produced by pyrolytic decomposition of CuO, ZnO, and NH_4Cl source powders. Heating of the source at 650 °C caused the formation of hexagonal ZnO crystallites with maximum diameters and heights up to tens of micrometers. Energy dispersive spectroscopy and selected area electron diffraction confirmed the synthesis of wurtzite structured ZnO, which was growing along the *c*-axis. ZnO crystallites were growing only in the presence of CuO in the source powder. We proposed that ZnO was nucleated from the molten copper chloride salts after over-saturating with Zn and oxygen. The further growth of ZnO was performed by the vapor phase growth using precursors formed after pyrolysis of source powders.

ZnO finds a wide range of applications in modern science starting with materials for electrical and optical devices and ending with bio-medical, pharmaceutical, and catalytic usage **[1 – 7]**. ZnO, which is a wide band-gap semiconductor, can be attributed to one of the most studied materials.

ZnO nanoparticles (NPs) with diameters below 100 nm have superior electrical, optical, biological, catalytic, and many other unique properties resulting from the large surface-to-volume ratio, domination of surface-related properties together with strong manifestations of size-dependent quantum effects.

ZnO NPs are synthesized by different technologies including chemical vapor deposition, plasma-enhanced methods, laser ablation, reactive sputtering, co-precipitation, sol–gel method, high energy ball milling, electrochemical and electrophoretic depositions, ultrasound, anodization, microwave-assisted, and combustion methods. Nowadays, ZnO NPs are also synthesized by biogenic methods using plants, yeast, fungi, bacteria, and algae **[8 – 12]**. As a rule, the properties and morphology of produced ZnO depend on the method of synthesis.

The purpose of this work was to present our preliminary results on the growth of ZnO micro- and nanocrystals using the new pyrolytic technology.

The details of developed technology can be found elsewhere **[13]**. In brief, it implies the formation of volatile Zn and copper molecules in the atmosphere of NH_4Cl thermal decomposition products. The source materials were chemically pure ZnO, CuO, and NH_4Cl powders. They were placed on the bottom of the evacuated vertical quartz tube which was heated in the temperature range of 400 – 700 °C through an external resistive furnace. The Si crystal substrate was located at 2 – 3 cm above the source material and heated by furnace radiation and convection. The samples were studied by scanning and transmission electron microscopy (SEM and TEM) using TESCAN Vega-3 XMU and Philips CM12 facilities.

The process parameters that may be varied during the synthesis were the source temperature, source substrate distance, the ratio of source powders. The results presented below concern the changes in morphology and composition of materials grown on Si substrate at two temperatures.

Figure 1 represents the SEM image and elemental map of particles that were formed on the surface of Si substrate after heating of ZnO + CuO source with the total mass of 1.8 g, mixed with 0.4 g NH_4Cl (18 wt. % NH_4Cl). Previously it was established that in the similar condition the separate treatment of CuO and ZnO powders cause the formation of Cu microcrystals in case of CuO source **[13]**, and Zn compounds when zinc oxide was used. The source was heated at 600 °C. As can be seen, the layer of microparticles with average sizes of 2 micrometer is produced. The segregation of copper particles is clearly shown in the EDS elemental map (**Figure 1b**). The formation of Cu particles is not surprising and complies with our previous results on the pyrolysis of CuO in ammonium chloride **[13]**. The distribution of other elements (Zn, oxygen, Cl) is rather homogeneous. It should be emphasized that the flat plains with perforated edges, denoted with arrow, can be observed in the central part of the image. They seem to be formed due to the coalescence of molten microparticle edges. The plate-like discs, denoted with asterisks, can be seen in the same region. Both of these structures do not contain copper, as is evidenced by the elemental map in **Figure 1b**.

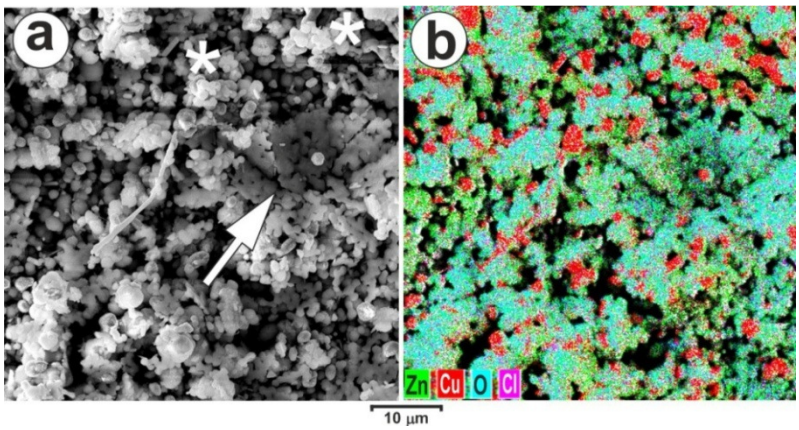

Figure 1. SEM image of layer formed on Si substrate after annealing of source powders at 600 °C **(a)** and elemental map of same area **(b)**.

The increase of a source temperature up to 650 °C causes the drastic changes in the morphology and structure of the synthesized product, as is represented in **Figures 2** and **3a**. The formation of hexagonal microcrystals with maximum diameters of ca. 20 micrometer can be

 https://doi.org/10.52340/ns.2020.12

observed. The surface distribution of crystals is quite random and their diameters are changed in the wide range. A part of them has an uncompleted hexagonal ring or comprises only part of a hexagon. The segregation of copper particles still presents, while the crystals contain mostly Zn and oxygen.

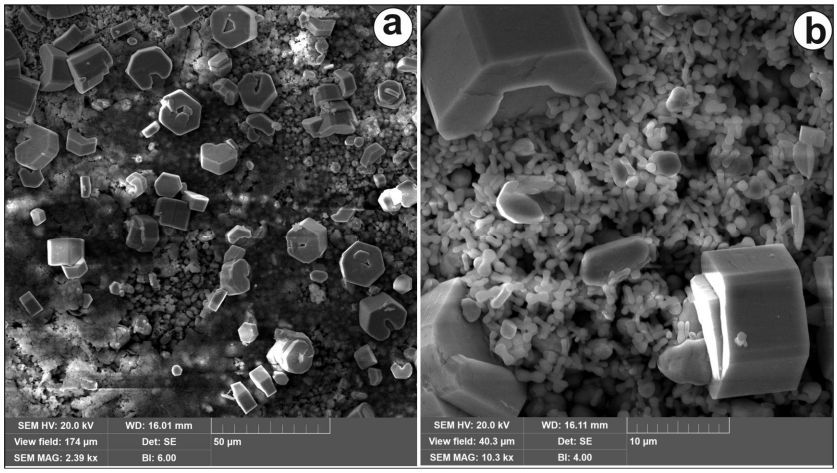

Figure 2. SEM images of materials produced on Si substrate after annealing of source at 650 °C; magnification: **(a)** × 2390 and **(b)** × 10300.

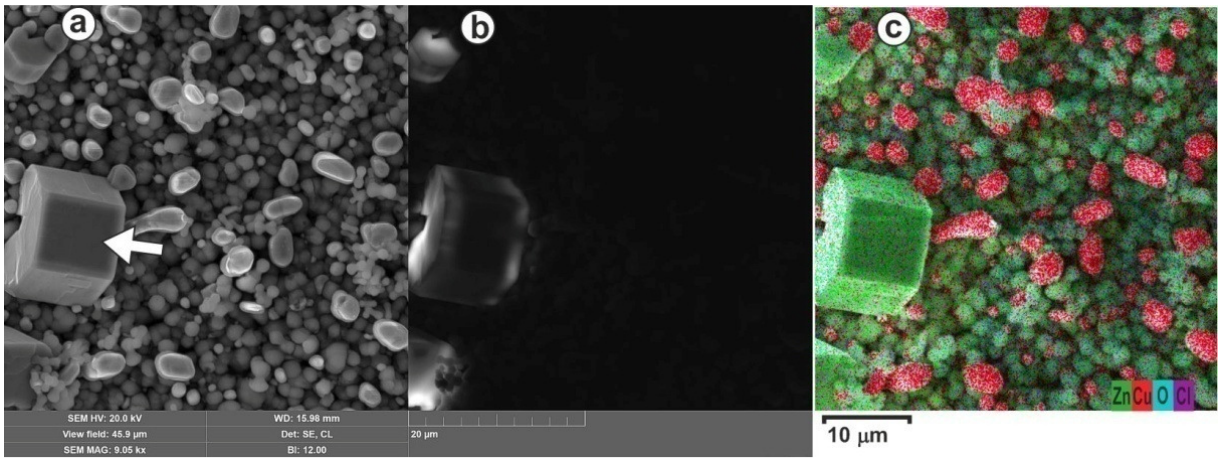

Figure 3. SEM and cathodoluminescence images of part of Si substrate covered with ZnO crystallites and microparticles **(a, b)** and elemental map of the same area **(c)**.

Table 1 lists the composition of synthesized materials. Data were collected using energy dispersive spectroscopy, which was attached to SEM facility. The compositions are presented as average content of elements over the areas shown in **Figures 1a** and **3a**. To obtain direct composition of a microcrystal, the electron beam was focused on one of its facet (prism plane) indicated by an arrow in **Figure 3a**. Data presented in **Table 1** clearly show that microcrystals consist of Zn and oxygen, and hexagonal ZnO is a most probable candidate for the composition of microcrystals. The excess of oxygen may be caused by its well-known adsorption on the surface of a sample after air exposure. Copper also exists in the microsrystalls. However, its concentration does not exceed 0.5 at. %, which is quite below of Cu solubility limit in ZnO (5 at. %. [**14**]). It should be emphasized that no ZnO microcrystal formation was observed without adding CuO powder in the source material.

Table 1. Composition of synthesized materials.

Element	Composition of area depicted in Figure 1a, at. %	Composition of area depicted in Figure 2a, at. %	Composition of crystal facet marked in Figure 2a, at. %
Zn	19.81	22.45	37.65
O	45.55	44.37	54.38
Cu	12.05	16.74	0.45
Cl	3.85	1.69	–
Si	13.25	7.73	–
C	5.50	7.09	7.52
Total	100	100	100

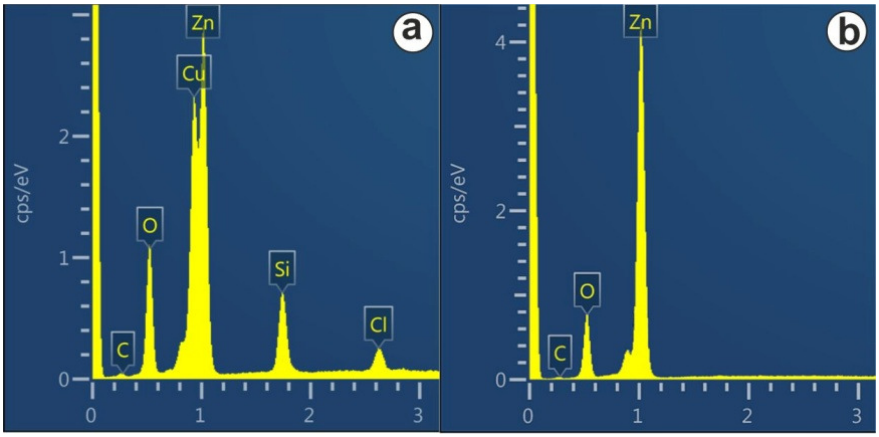

Figure 4. EDS peaks obtained from whole area presented in **Figure 3a (a)** and from crystallite indicated with arrow **(b)**.

Figure 4 demonstrates the difference between the overall composition of the area depicted in **Figure 3a** and the composition of the microcrystal marked by an arrow. The peaks of Cu, Cl, and Si are almost completely eliminated.

The cathodoluminescence (CL) image of the area presented in **Figure 3a** is shown in **Figure 3b**. The luminescence is observed only for hexagonal microcrystals proving that the material of microcrystals may have a direct band gap. The last fact can be considered as another approval of the formation of a wurtzite structured ZnO as it has a direct band gap.

TEM image of a microcrystal is presented in **Figure 5** together with the Selected Area Electron Diffraction (SAED) pattern. The calculated interplanar spacings proved once again the formation of wurtzite ZnO (JCPDS card N 036–1451).

One of the major subjects of crystal formation is the nucleation and growth mechanisms. More complex further investigation is needed to clarify these items. However, we can make some assumption based on the obtained results. EDS data illustrate that this material contains Zn, Cu, Cl, and O. The salts like CuCl, $CuCl_2$, or copper oxychloride – $Cu_2(OH)_3Cl$ can be produced on the Si substrate from precursors that were formed after pyrolysis of source powders. The listed compounds have low melting points ranging from 250 °C for oxychloride, up to 498 °C for $CuCl_2$. During our growth process, the surface of Si substrate may attain these temperatures. The blurred regions shown at the bottom of **Figure 3** can be possibly attributed to

https://doi.org/10.52340/ns.2020.12

the solidified molten salt, which may serve as Zn vapor sink. The molten salt growth method is a well established technology for the growth of crystalline materials **[15 – 17]**. We suppose that after oversaturation with Zn and O, the salt may facilitate the formation of ZnO nuclei, which may then grow either by molten salt method or by vapor phase epitaxy.

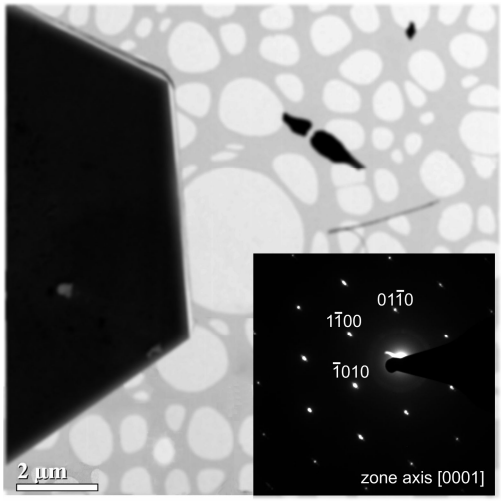

Figure 5. TEM image of thin ZnO plate. Inset
Shows Selected Area Electron Diffraction pattern.

In conclusion, we have shown that ZnO microcrystals can be grown using ZnO, CuO, and NH_4Cl powders as source materials. Annealing of the source at 650 °C causes the formation of volatile species, which produce on Si substrate the layer of Cu, Zn, Cl, and O containing microparticles. It is suggested, that ZnO is produced from Cu chlorides or copper oxychloride molten salts, after their oversaturation with zinc and oxygen. The microcrystals with diameters up to tens of micrometers were grown along the *c*-axis and they have the hexagonal wurtzite structure.

Acknowledgement

This work was supported by Shota Rustaveli National Science Foundation of Georgia (SRNSFG) – Grant Number YS–19–087.

References

[1] V. Parihar, M. Rajam, R. Paulose. Rev. Adv. Mater. Sci., 2018, 53, 119.
[2] A. N. Ul Haq, A. Nadhman, I. Ullah, G. Mustafa, M Yasinzai, I. Khan. J. Nanomater., 2017, 8510342, 1-14.
[3] A. Kołodziejczak–Radzimska, T. Jesionowski. Mater., 2014, 7, 2833.
[4] T. C. Bharat, S. Mondal, H. S. Gupta, P. K. Singh, A. K. Das. Mater. Today, 2019, 11, 767.
[5] H. Zheng, D. Wu, Y-L. Wang, X.-P. Liu, P.-Z. Gao, W. Liu, J. Wen, E. V. Rebrov. J. Alloys Comp., 2020, 838,155219.
[6] X. Shen, H. Shao, Y. Liu, Y. Zhai. J. Mater. Sci. Technol., 2020, 51, 1.
[7] N. Tiwale. J. Mater. Sci. Technol., 2015, 31,14, 1681.

[8] Inamuddin, N. Shakeel, A. Imran, S. Kanchi, H. A. Kashmery. Sci. Rep., 2020, 10, 5052.
[9] A. Aldalbahi, S. Alterary, R. A. A. Almoghim, M. A. Awad, N. S. Aldosar, S. F. Alghannam, A. N. Alabdan. Molecules, 2020, 25, 4198.
[10] J. Santoshkumar, V. Kumar, R. Shanmugam. Resource-Efficient Technologies, 2017, 3, 4, 459.
[11] R. Sharma, R. Garg, A. Kumari. EXCLI J., 2020,19, 1325.
[12] K. Sadowska. Biotechnologia, 2014, 2, 2, 150.
[13] D. Jishiashvili, Z. Shiolashvili, N. Makhatadze, A. Jishiashvili, A. Chirakadze, V. Gobronidze. Nano Studies, 2019, 19, 285.
[14] S. Das, V. C. Srivastava. Nanotechnol. Rev., 2018, 7, 3, 267.
[15] P. Afanasiev. J. Phys. Chem. C, 2012, 116, 2371.
[16] X. Wang, H. Yin, W. Liu, G. Yu, J. He, Z, Tang, L. Yan. Materials and Corrosion, 2019, 1.
[17] T. A. Rozdyalovskaya. Russian Metallurgy (Metally), 2018, 2, 163.

 https://doi.org/10.52340/ns.2020.12